ACS OMEGA

http://pubs.acs.org/journal/acsodf

Article

Re-examination of Peptide-Sequence-Dependent Gene Expression of Cysteine-Installed Pegylated Oligolysine/DNA Complexes

Yuichi Yamasaki,* Daiki Kumekawa, Satoshi Yamauchi, and Hodaka Omuro

Cite This: *ACS Omega* 2022, 7, 15478−15487

Read Online

ACCESS | Metrics & More | Article Recommendations | Supporting Information

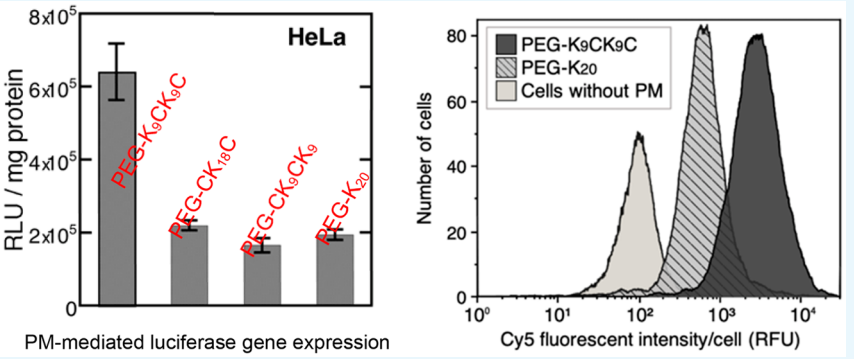

ABSTRACT: We previously synthesized cysteine-installed C-terminally PEGylated oligolysines with 20 amino acid residues to form cross-linked polymeric micelles (PMs) with luciferase-coding plasmid DNA as a candidate for artificial gene vectors. Luciferase gene expression in HeLa cells mediated by PEG−$CK_{18}C$, PEG−CK_9CK_9, and PEG−K_9CK_9C was reported to be 35-, 5.4-, and 1.3-fold higher than that mediated by cysteine-uninstalled PEGylated oligolysine PEG−K_{20}, respectively. However, after the publication, the survival rate of HeLa cells used in the previous study was found to be lower than usual when subcutaneously implanted into mice to create a xenograft model. In this study, to re-examine the peptide sequence-dependent gene expression, gene expression efficacy mediated by PEG−peptide PMs was compared with the PM cellular uptake results using newly obtained HeLa cell lines and the additional cell lines Huh-7, PANC-1, and BxPC3. As a result, PEG−K_9CK_9C PMs mediated the maximum gene expression in all cell lines, and the corresponding cellular uptake was also obtained. Therefore, we concluded that our previous results were erroneously obtained due to normality-depleted HeLa cells. A comparison of physicochemical characterizations, gene expression efficacy, and cellular uptake of PEG−peptide PMs is discussed in detail.

INTRODUCTION

PEGylated peptides[1−3] and PEGylated polypeptides[4−6] are treated as artificial gene vector backbones for gene therapy. In many cases, the peptide-based gene vector backbone is mainly composed of basic amino acids, lysine, or arginine. A few successful examples of 10 kDa PEG-substituted lysine 30-mer CK30PEG10k that mediated transgene expressions in both alveolar and airway epithelium mice cells via intratracheal or intranasal instillation[37] and in rat brains via intranasal administration[38] were reported. The former led to clinical trials for cystic fibrosis transmembrane regulator gene transfer and resulted in the desired expression at the nasal mucosa of the inferior turbinate.[39] On the other hand, the realization of gene expression at target organs via systemic intravenous administration is still a challenging goal. Considerable efforts have been devoted to synthesizing improved gene transfer systems with high efficiency because artificial vector systems, including polyplexes and lipoplexes, generally show low expression regardless of being safer than virous systems.[7,8] To enhance gene expression efficacy, ligand conjugation for specific cells has often been employed to formulate delivery systems.[9−11]

Functionalization by installing cell-targeting ligands and intracellular signals in a multilayered manner is an advantage of synthetic polyplex systems,[12] whereas another strategy is to explore the specific sequence of DNA-binding peptides to enhance gene expression efficacy. For this purpose, PEGylated peptides synthesized by solid-phase peptide synthesis (SPPS) seem preferable because SPPS can offer a singly defined sequence suitable for the correlational study of peptide sequences and bioactivities.[13] On the contrary, PEGylated polypeptides prepared by polymerization of *N*-carboxyanhydride (NCA) of amino acids (NCA polymerization) have

Received: January 7, 2022
Accepted: April 8, 2022
Published: April 27, 2022

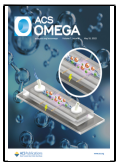

heterogeneity in the degree of polymerization (DP) and face difficulties in precisely arranging amino acid sequences.[13,14] For example, systematic studies on PEG−poly(L-lysines) (PEG−PLL)[6] and unconjugated PLL[15] prepared by NCA polymerization showed no correlation between the average DP of PLL and *in vitro* gene expression efficacy.

Peptide-based polyplex systems have had their structure−activity relationship successfully demonstrated in a comparative study between clustered $(KKKHHHHKKK)_6$ and dispersed $(KHKHKHKHKK)_6$ peptides fused to a fibroblast growth factor, where the former exhibited 6-fold higher transfection efficiency.[16] A similar trend was observed in gene expression mediated by sequence-regulated poly(histidine-*co*-lysines), poly(H_8K_4), poly[$(HHK)_4$], poly[$(KKH)_4$], and poly[$(HK)_6$].[17] Although the interaction of protonated histidines and endosomal membranes that is believed to be key for endosomal release of polyplexes is still under debate, contiguous sequences of trimeric histidines H_3 or longer enhanced gene expression efficacy in many cases of histidylated oligolysines prepared by SPPS.[16−18]

The modulation of peptide sequences by adding other amino acids can enhance gene expression efficacy, as shown in the above examples. Another example was reported in *in vitro* reporter gene expression mediated by C-terminally PEGylated cysteine-containing oligolysine peptides.[19] We reported that gene expression in HeLa cells mediated by PEG−$CK_{18}C$, PEG−CK_9CK_9, and PEG−K_9CK_9C was 35-, 5.4-, and 1.3-fold higher, respectively, than that mediated by cysteine-uninstalled PEGylated oligolysine PEG−K_{20}. On these PEG−peptides, the positions of cysteines introduced were chosen as special positions from the viewpoint of polymer segment mobility. In this case, cysteine residues were incorporated to form cross-linked polyplex micelles (PMs) by disulfide bonds and to facilitate intracellular DNA release due to reductive environment-responsive disulfide cleavage. However, the mechanism of peptide-sequence-dependent gene expression remains unknown.

In addition, the survival rate of HeLa cells used in the previous study was found to be lower than usual when subcutaneously implanted into mice to create a xenograft model—this was observed after publication. We seriously considered this fact and decided to re-examine the sequence dependency in the PEG−peptide PM-mediated gene expression using newly obtained HeLa cells and several other cell lines. Although a complete understanding of the mechanism of peptide-sequence-dependent gene expression is difficult, in an attempt to find evidence of cellular response to the above PMs, reporter gene expression efficacy and cellular uptake in HeLa, Huh-7, PANC-1, and BxPC3 cell lines were evaluated in this study. These four cell lines that are subcutaneously transplantable to create mouse xenograft tumor models were chosen for the *in vivo* experiments in the future work.

We confirmed a different trend of sequence-dependent reporter gene expression mediated by the cross-linked PMs in all the studied cell lines. The highest gene expression was observed in the expression mediated by PM composed of PEG−K_9CK_9C in all cell lines, and this trend differed from our previous study. In the present study, the EtBr dye exclusion assay, gel electrophoresis retardation assay, and TEM observations were carried out as preliminary characterizations of PMs. A detailed discussion is provided by comparing gene expression efficacy and cellular uptake of cross-linked PMs formulated by cysteine-installed PEGylated oligolysines.

EXPERIMENTAL SECTION

Materials. α-Methoxy-ω-amino-PEG (MeO-PEG-NH_2, M_n = 12 kDa, M_w/M_n = 1.02) was obtained from NOF (Tokyo, Japan). N-Protected amino acids were obtained from Merck (Darmstadt, Germany). 1-Hydroxybenzotriazole hydrate (HOBt), *N*,*N*′-diisopropylcarbodiimide, and triisopropylsilane (TIS) were purchased from Sigma-Aldrich (St. Louis, MO). Dithiothreitol (DTT) was purchased from Nacalai Tesque (Tokyo, Japan). Plasmid DNA Col E1 was purchased from Nippon Gene (Toyama, Japan). Luciferase-coding plasmid DNA pCAG-luc2 (6477 bp) and human hepatoma cell line Huh-7 were obtained from RIKEN Bioresource Research Center (Tsukuba, Japan). This pDNA was amplified in competent DH5α *Escherichia coli* cells, followed by extraction and purification using the NucleoBond Xtra Maxi Plus EF (Macherey-Nagel, Duren, Germany). pDNA was later reconstituted in 10 mM HEPES buffer (pH 7.4). Two types of human pancreatic adenocarcinoma cell lines, PANC-1 (liver nonmetastatic) and BxPC3 (highly liver metastatic), were provided by the American Type Culture Collection (Manassas, VA). HeLa cells were a gift from Prof. Toshiya Sakata of the University of Tokyo.

PEGylated Peptides. C-terminally PEGylated peptides used in the previous report[19] were employed in the current work. Briefly, protected peptides were synthesized using Fmoc-based SPPS on 2-chlorotrityl resins (Advanced ChemTech, Louisville, KY) in *N*-methyl-2-pyrrolidone using a peptide-synthesizing shaking apparatus (KMS-3, Kokusan Chemical, Yokohama, Japan). Fmoc-protected and Boc-protected amino acids were used for peptide elongation and the N-terminal, respectively. To obtain protected peptides, 25% hexafluoro-2-propanol dichloroethane solution was applied for 2 h at room temperature. The protected peptides were confirmed by electrospray ionization mass spectrometry (ESI-MS, micro-TOF, Bruker Daltonics, Bremen, Germany) in negative mode and ^{1}H NMR (JNM-ECS400, JEOL, Tokyo, Japan). PEGylation was performed using a method similar to that used for peptide elongation. After the PEGylation, an excess amount of unreacted peptide was removed by the preparative GPC (HLC-8220GPC, Tosoh, Tokyo, Japan). GPC conditions and all GPC charts of purified protected PEG−peptides are given in the Supporting Information (Figures S1−S4). Other characterizations of PEG−peptides were reported previously.[19]

In this study, PEG−K_9CK_9C, PEG−$CK_{18}C$, PEG−CK_9CK_9, and PEG−K_{20} were used as PEG−peptides. As described in the Introduction, cysteines were inserted at two positions of N-terminal, C-terminal, or the center of peptides as typical positions from the viewpoint of polymer segment mobility. The mobility of the terminal residue of the polymer chain is greater than that of other residues.[42] The residue connecting to PEG also possesses different mobility from inner residues because all residues except for both peptide terminals have electrostatically anchoring residues at both neighbors.

Generally, reducing agents can cleave disulfide bonds localized at the surface where solvent molecules are accessible. Disulfide bonds inside the protein are hardly cleavable even by tributylphosphine which is a stronger reductant than DTT without the help of denaturing agents like urea.[43] Therefore, disulfide bonds inside the PM's core are hardly cleavable

https://doi.org/10.1021/acsomega.2c00122
ACS Omega 2022, 7, 15478−15487

Table 1. Morphometric Characteristics for the Histogram of PM Rod Length Observed in TEM Images (Figure 4)[a]

	PEG−K_9CK_9C	PEG−$CK_{18}C$	PEG−CK_9CK_9	fPEG−K_{20}
mean rod length (SD)/nm	342.6 (104.7)	328.4 (95.8)	377.4 (109.5)	217.2 (84.4)
mode[b]/nm	310	310	310, 330	210
<200 nm/count	6	9	1	47
ring-shaped[c]/%	7.6	16.3	28.6	24.2
mean surface area/nm^2	8385	8215	8787	6749
PEG density/chains/nm^2	0.081	0.083	0.076	0.091

[a]n = 100 for rod-like PMs. [b]Expressed by the central value of each class (class interval is 20 nm). [c]Deduced from the number of ring-shaped PMs observed in measuring rod-like PMs up to 100.

similarly. Considering that the formation of a disulfide bond is an equilibrium reaction, the disulfide bonds possessing a high degree of freedom of mobility are thought to be more exchangeable. We thought that these complicated interactions might be related to peptide sequence differences and that they can modulate the PM's stability or pDNA release property both inside and outside the cell.

Preparation of Cross-Linked PMs. PEG−peptides were dissolved in 10 mM HEPES (pH 7.4), and to cleave any preformed disulfide bonds an appropriate amount of DTT stock solution (100 mM) was added so that the final DTT concentration became 10 mM. The solutions were allowed to stand for 30 min at room temperature. PMs were then prepared at a ratio of positive charges of the polymer to DNA phosphate negative charges (N/P ratio) of 2.0 or as desired by fast mixing of the PEG−peptide solutions with an adequate quantity of pDNA stock solution. To remove DTT, double dialysis using a Mini Dialysis kit (8 kDa cutoff; GE Healthcare Japan, Tokyo, Japan) was carried out against 10 mM HEPES containing 0.5% (v/v) DMSO for 24 h for the first dialysis and 10 mM HEPES for 48 h for the second. The final pDNA concentration for PM formulation was adjusted to 20.0 μg/mL for the agarose gel electrophoresis or to 33.3 μg/mL for TEM observation and the *in vitro* assay. The disulfide bond formation of cross-linked PMs was confirmed by Ellman's method.[20]

EtBr Dye Exclusion Assay. A sample solution containing 1.0 μg/mL of pDNA and 0.5 μg/mL of EtBr was titrated using the PEG−peptide solution until the maximum N/P ratio was 10.0. Both solutions contained 10 mM DTT to avoid dimerization of PEG−peptides. The fluorescence intensity of EtBr excited at 510 nm was measured at 590 nm at fixed N/P ratios using a spectrofluorometer (FP-8300; Jasco, Hachioji, Japan). The relative fluorescence intensity F_r is defined as follows

$$F_r = (F_{sample} - F_0)/(F_{100} - F_0)$$

where F_{sample} is the sample fluorescence intensity; F_{100} is the intensity measured at N/P = 0; and F_0 is the background intensity.

Agarose Gel Electrophoresis. Agarose gel (0.9%) was prepared, and electrophoresis was performed at 100 V for 30 min in 3.3 mM TAE buffer (pH 7.4). When the PM stability under physiological salt concentration was evaluated, the PM samples were left to stand in the desired salt concentration for 24 h before electrophoresis. Similarly, a reductive environment-responsive pDNA release was evaluated by preincubation with 10 mM DTT for 24 h. Immediately after electrophoresis, the gel was stained with 0.5 μg/mL of EtBr for 30 min and washed in water for 30 min, followed by observation on an UV transilluminator. PM stability was also assessed by the polyanion exchange reaction, which was carried out by adding sodium dextran sulfate (M_w = 500 kDa) to the PM solution. PM solutions (10 μL, 33.3 μg/mL of DNA) were mixed with an adequate volume of sodium dextran sulfate solutions in 10 mM HEPES buffer with 150 mM NaCl. The ratios of sodium dextran sulfate to DNA (S/P ratio) were set to 0, 2.0, 3.0, and 5.0. Each sample was electrophoresed after 2 h of incubation at 37 °C.

TEM Characterization. PM morphology was observed using a JEM-1400 transmission electron microscope (JEOL) operated at 120 kV. Carbon-coated copper grids with a collodion film (JEOL) were hydrophilized using a hydrophilic processor (DII-29020HD, JEOL). On the hydrophilized grids, 2 μL each of uranyl acetate (2% w/v) and PM solutions were mixed and allowed to stand for 30 s. Sample-deposited grids were blotted onto filter paper to remove excess solution. Rod-like pDNA condensates were observed as the major PM morphology, whereas ring-shaped PMs were minor. The long-axis length of rod-like PMs was measured on TEM images using ImageJ 1.47 software.[21] A hundred rod-like PMs were measured to plot the rod length distribution of each PM.

***In Vitro* Gene Expression Assay.** HeLa, Huh-7, and PANC-1 cells were seeded onto 24-well plates (50 000 cells/well) and incubated at 37 °C in 5% CO_2 for 24 h in 400 μL of DMEM medium (Wako Pure Chemical, Tokyo, Japan) containing 9% fetal bovine serum (Thermo Fisher Scientific, Waltham, MA) and 0.9% penicillin-streptomycin (Thermo Fisher Scientific). For BxPC3 cell proliferation, the RPMI-1640 medium was used instead of DMEM, and other conditions were the same as above. Immediately after the medium change, a PM solution containing 1 μg of pCAG-Luc2 pDNA was added to each well and incubated for 24 h. After the medium was changed again, the cells were incubated for another 24 h. Then, all media were removed, and the cells were washed twice with 200 μL of phosphate-buffered saline (Wako Pure Chemical). After 20 min of incubation with 150 μL of passive lysis buffer (Promega, Madison, WI) at 37 °C, 20 μL of the lysate was mixed with 100 μL of luciferase assay reagent, and luciferase gene expression was evaluated by measuring luminescence intensity using a Mithras LB 940 multimode microplate reader (Berthold Technology, Bad Wilbad, Germany). Additionally, the expressed protein was quantified using the Micro BCA protein assay reagent kit (Thermo Fisher Scientific), and transfection efficacy was represented as relative light units/mg of protein. Note that the background value was subtracted from each datum (n = 4).

Cellular Uptake Assay. Plasmid DNA pCAG-luc2 was fluorescently labeled using a *Label* IT Tracker Cy5 kit (Mirus Bio, Madison, WI) according to the manufacturer's protocol. HeLa and BxPC3 cells were seeded using the same protocol described above. After removal of the PM-containing medium,

https://doi.org/10.1021/acsomega.2c00122
ACS Omega 2022, 7, 15478−15487

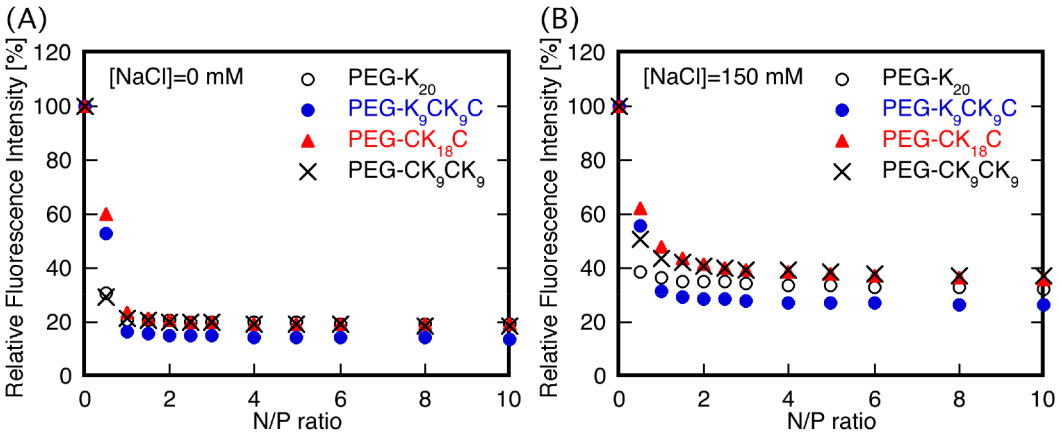

Figure 1. Relative binding affinity of PEG−peptides to pDNA in the absence (A) or presence (B) of salt. PEG−K_{20} (open circle), PEG−K_9CK_9C (blue circle), PEG−$CK_{18}C$ (red triangle), and PEG−CK_9CK_9 (cross).

the cells were treated with a trypsin−EDTA solution. The corrected cells were washed with PBS through centrifuge separation and resuspension. Suspended cells were injected into a cell sorter (FACSAria III, BD Bioscience, Franklin Lakes, NJ), and fluorescence from cells containing Cy5-labeled pDNA excited at 633 nm was detected (n = 10 000).

Statistical Analyses. Distributions of PM rod length observed in TEM images are expressed by their histogram (Figure 4). Mean rod lengths are reported with their corresponding standard deviation (SD) (Table 1). PM-mediated gene expressions (Figure 6) were analyzed using a one-way analysis of variance (ANOVA) with a post hoc Tukey honesty significant difference (HSD) test. The statistical significance was set at $^*p < 0.05$. Means are reported with their corresponding standard error (SE).

RESULTS AND DISCUSSION

PM Formation. Prior to the physicochemical characterization of PMs, the binding affinity of PEG−peptides to pDNA Col E1 was tested using an EtBr dye exclusion assay (Figure 1) and an agarose gel electrophoresis retardation assay (Figure 2). In the EtBr dye exclusion assay, the PEG−peptide binding ability to pDNA can be exemplified by measuring the decrease in the fluorescence intensity of EtBr. This decrease in fluorescence intensity reflected the release of intercalated EtBr from pDNA upon PEG−peptide binding. As shown in Figure 1, when the N/P ratio increased, the EtBr fluorescence intensity sharply decreased at the initial stage N/P < 1.0, followed by a plateau region despite the presence or absence of added salt. This result is in close agreement with our previous work.[19]

A gel retardation assay was conducted in the case of PEG−K_{20} as a typical example in the presence of 150 mM NaCl. The gel electrophoretic mobility of pDNA also qualitatively reflects the binding of PEG−peptides to pDNA. As shown in Figure 2, pDNA mobility decreased sharply in the region of N/P < 0.75, and pDNA migration was not detected with a further increase in PEG−K_{20}. This trend is consistent with the EtBr dye exclusion assay results, as shown in Figure 1, and the zeta potential measurement results of our previous work.[19] In the range of tested N/P ratios, a charge-inverted PM[22,23] that occurs with the presence of excess cations and migrates toward the opposite direction was not detected, suggesting that PMs composed of PEG−peptides were formulated as charge-

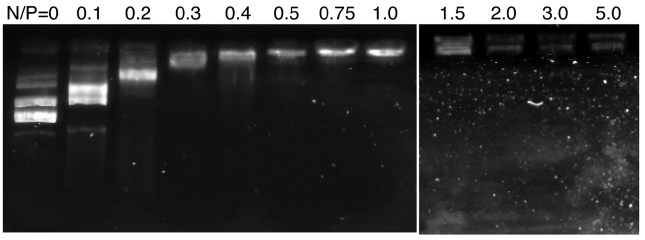

Figure 2. Agarose gel electrophoresis to assess the PM formulation in the case of PEG−K_{20} in the presence of 150 mM NaCl.

neutralized pDNA condensates in the presence of added salt. Based on these characterizations, the N/P ratio was set at 2.0 as a standard condition.

As for PM morphology, TEM observation was performed on negatively stained PMs using uranyl acetate. A pDNA pCAG-Luc2 (6477 bp, total length: 2202 nm) was used for further experiments described below. As exemplified by the TEM image of PMs composed of PEG−CK_9CK_9 shown in Figure 3, both rod- and ring-shaped PMs were observed as being major and minor in all samples, respectively. The percentage of ring-shaped PMs was less than 30%, as indicated in Table 1. The rod length distributions for all the PMs were evaluated using a

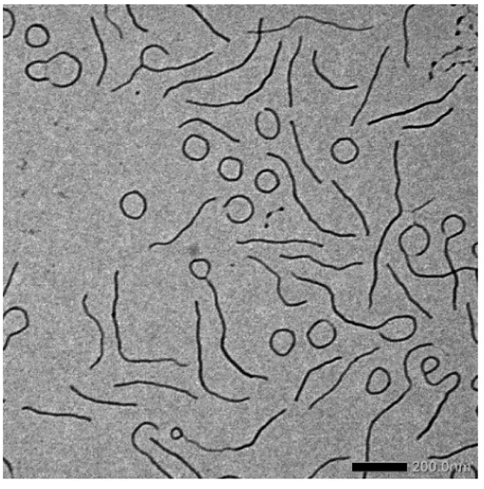

Figure 3. TEM image of cross-linked PMs composed of PEG−CK_9CK_9. The scale bar indicates 200 nm.

https://doi.org/10.1021/acsomega.2c00122
ACS Omega 2022, 7, 15478−15487

histogram analysis, as shown in Figure 4. The contour length of DNA measured from TEM images was somewhat shortened, as previously reported.[24]

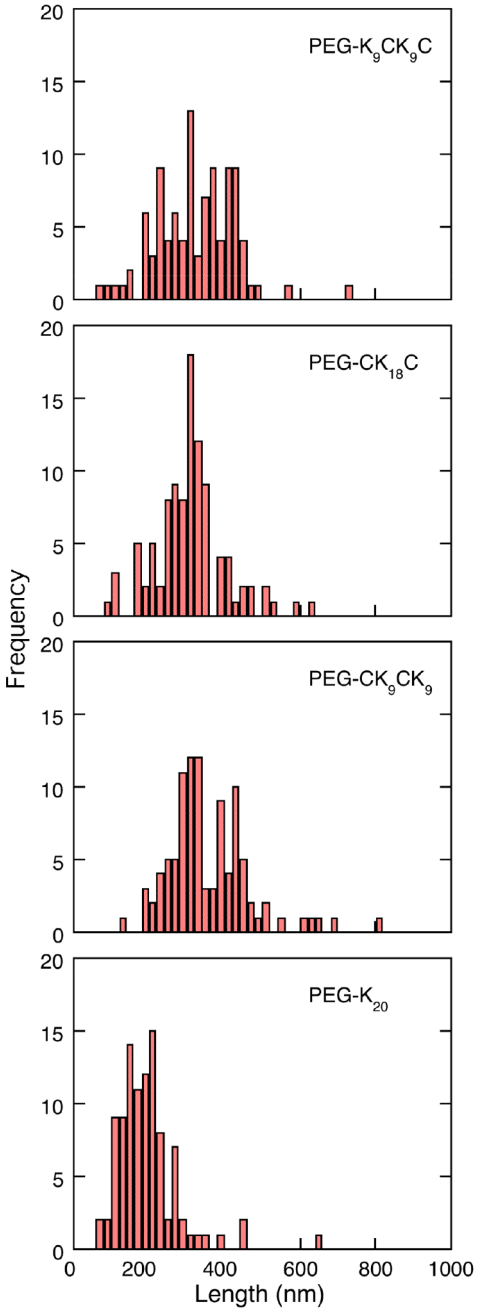

Figure 4. Rod length distribution analyzed from TEM images. n = 100 in each PM sample, [NaCl] = 150 mM.

In the cross-linked PMs, the greatest frequency in the rod length distributions was found in the range from 300 to 340 nm, and highly folded PMs with rod lengths shorter than 200 nm were significantly fewer (Figure 4 and Table 1). These trends in rod length distributions of cross-linked PMs were consistent with our previous work.[19] However, the rod length distribution of non-cross-linked PMs composed of PEG−K_{20} remarkably differed from those of other cross-linked PMs. The number of PMs with rod lengths shorter than 200 nm reached almost half the population of non-cross-linked PMs composed of PEG−K_{20}. This difference might be somewhat influenced by the type of pDNA used. pCAG-Luc2 was employed in this work, and the previous one was model pDNA Col E1.

More specifically, the percentages of rod-like PMs longer than 400 nm in PEG−K_9CK_9C PMs and PEG−CK_9CK_9 PMs were 26 and 30%, respectively, which were slightly more than that in PEG−$CK_{18}C$ PMs (14%). In contrast, in PEG−$CK_{18}C$ PMs, PMs shorter than 360 nm accounted for 82%. Although the size was not measured, the ratio of ring-shaped PMs observed during the measurement of rod-like PMs was quite different depending on the peptide sequence. These values were somewhat lower than those in our previous work and possibly affected by the difference in pDNA employed.

PM Functionality. In our system, two cysteine residues were incorporated into PEG−peptides to equip PMs to release pDNA in response to the intracellular reductive environment but were stable outside the cells. Therefore, both PM stability in the physiological salt solution and pDNA-release properties under reductive conditions that mimic an intracellular environment should be evaluated.

These two properties of PMs were examined by a gel electrophoresis retardation assay in the presence of dextran sulfate as a model polyanion because negatively charged polysaccharides such as heparan sulfates were reported to inhibit polyplex-[25] and lipoplex-mediated[26] *in vitro* transfection. Additionally, dissociation of polyplexes was suggested at the kidney glomerular basement membrane[27] and in the extracellular matrix of the liver,[28] which are both bound to heparan sulfate proteoglycans. Thus, their interactions with polyplexes are suspected to affect the efficacy of polyplex-mediated gene delivery.

Therefore, sodium dextran sulfate was added to the PM solutions at different charge ratios, the ratio of the sulfate groups of dextran sulfate to pDNA phosphates (S/P ratio), and the sample solutions were allowed to stand for 2 h before electrophoresis. As a result, in the absence of DTT (right series of Figure 5), all cross-linked PMs maintained their complexed forms at any S/P ratio in the presence of added salt, whereas PMs composed of PEG−K_{20} released pDNA at S/P = 5.0.

Under reductive conditions (left series of Figure 5), all cross-linked PMs released pDNA depending on the S/P ratio in the presence of 10 mM DTT. This result indicates that incorporating cysteine residues into PEG−oligolysines contributed to the functionalization of intracellular reductive environment-responsive pDNA release into PEG−peptide PMs. The S/P ratio dependency observed in the pDNA-release property reflected the PM stability that was affected by the peptide sequence of PEG−peptides. This dependency indicates that PMs composed of PEG−K_9CK_9C and PEG−$CK_{18}C$ (lanes 1 and 2, respectively) were robust PMs, consistent with our previous work.[19] From the viewpoint of physicochemical characterizations, the reproducibility of PM formation with cysteine-installed PEG−oligolysines was firmly confirmed.

The stability of PMs against DNase or serum was also assessed by a gel electrophoresis retardation assay. pDNA fragmentation was confirmed against DNase, but the degree of pDNA fragmentation was similar in all PM samples (runs #1 and #2 of Figure S5 in the Supporting Information). For the PM stability against serum, whereas non-cross-linked PMs (PEG−K_{20} PMs) easily released pDNA, all cross-linked PMs were equally stable (runs #3 and #4 of Figure S5 in the Supporting Information). To release pDNA from all cross-

https://doi.org/10.1021/acsomega.2c00122
ACS Omega 2022, 7, 15478−15487

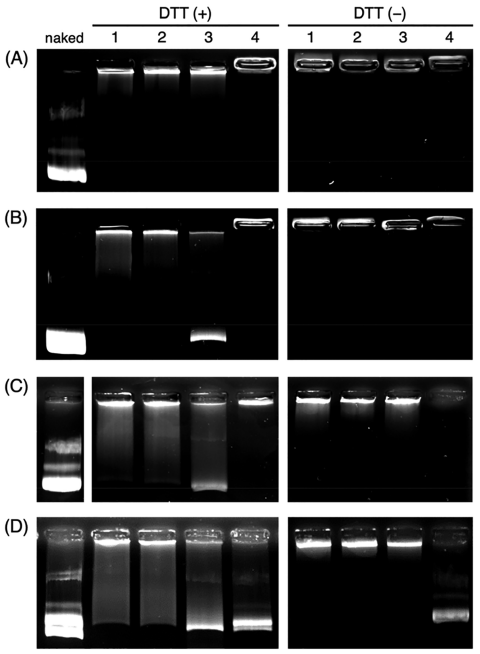

Figure 5. PM stability assessed by the polyanion exchange reaction by adding sodium dextran sulfate with (left) or without (right) DTT. The ratios of sodium dextran sulfate to DNA (S/P ratio) were set to 0 (A), 2.0 (B), 3.0 (C), and 5.0 (D). Lanes 1: PEG−K_9CK_9C; lanes 2: PEG−$CK_{18}C$; lanes 3: PEG−CK_9CK_9; and lanes 4: PEG−K_{20}. All the sample solutions were prepared in the presence of 150 mM NaCl.

linked PMs, a ten times higher DTT concentration was finally employed in the additional experiment (run #5 of Figure S5 in the Supporting Information). Against FBS, all cross-linked PMs were stable, and pDNA fragmentation was not observed. Additionally, to confirm the PM stability prior to and after the incubation in serum, DLS measurements were conducted. From DLS measurements, the colloidal stability of all PMs was confirmed, and aggregation was not detected even after 24 h of incubation with the presence of 10% FBS (Figures S6−S9 in the Supporting Information). Therefore, there is no significant difference in the stability of cross-linked PMs.

***In Vitro* Luciferase Gene Expression in Different Cell Lines.** A comparison of PM-mediated gene expression efficacy in different cell lines was assessed to re-examine the peptide-sequence-dependent gene expression observed in HeLa cells in our previous study,[19] and the presence or absence of cell line dependency in gene expression was also evaluated using the additional cell lines Huh-7, PANC-1, and BxPC3. These four cell lines were chosen for the *in vivo* experiments in future work.

From Figure 6, one can see that PEG−K_9CK_9C PMs showed the highest gene expression in each cell line. Gene expression efficacy mediated by PEG−K_9CK_9C PMs was 2- to 8-fold greater than that of other PMs. While a one-way ANOVA did not recognize the significance in PM-mediated gene expression in BxPC3 cells [$F(4,19) = 1.74$, $p = 0.19$], those in other cell lines showed significant results: Huh-7 [$F(4,19) = 11.61$, $p < 0.001$], HeLa [$F(4,19) = 8.32$, $p < 0.001$], and PANC-1 [$F(4,19) = 8.11$, $p = 0.0011$]. The highest gene expression mediated by PEG−K_9CK_9C PMs in these three cell lines with statistical significance $p < 0.05$ was also confirmed by ANOVA with a posthoc Tukey HSD test. Among gene expressions mediated by PEG−$CK_{18}C$, PEG−CK_9CK_9, and PEG−K_{20}, significant differences were not recognized by ANOVA in all cell lines. When Lipofectamine 2000 was used for comparison, the gene expression efficacy

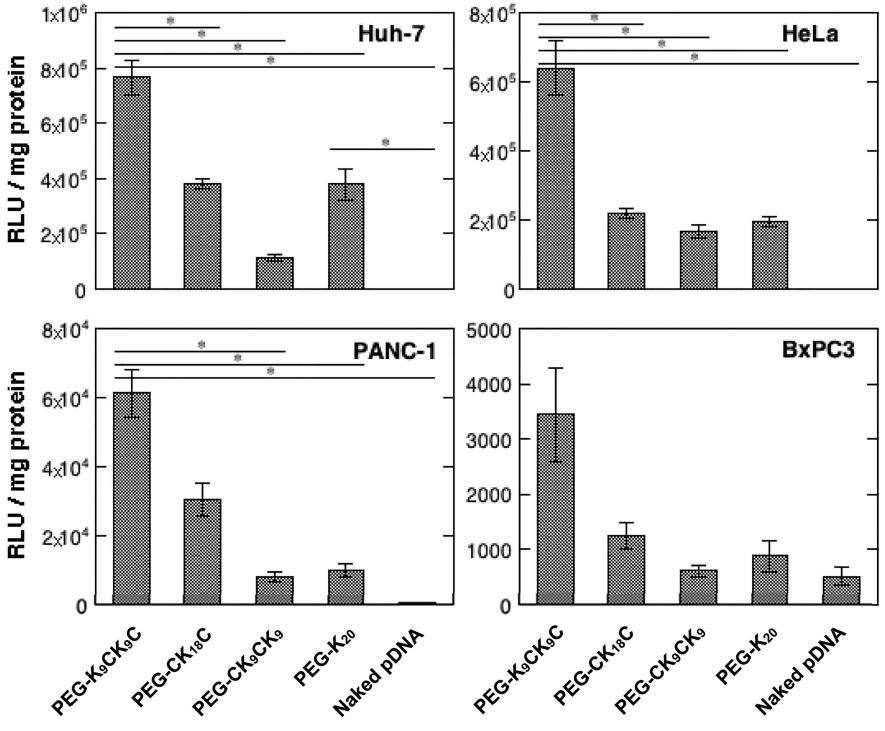

Figure 6. Cell line dependency in PM-mediated *in vitro* gene expression efficacy ($n = 4$, mean ± SE). The data are expressed as relative light units (RLUs) and an arbitrary unit (AU), and the background value was subtracted from each datum. A one-way ANOVA with post hoc Tukey HSD test was used for the statistical analysis. The statistical significance was set at $^*p < 0.05$.

https://doi.org/10.1021/acsomega.2c00122
ACS Omega 2022, 7, 15478−15487

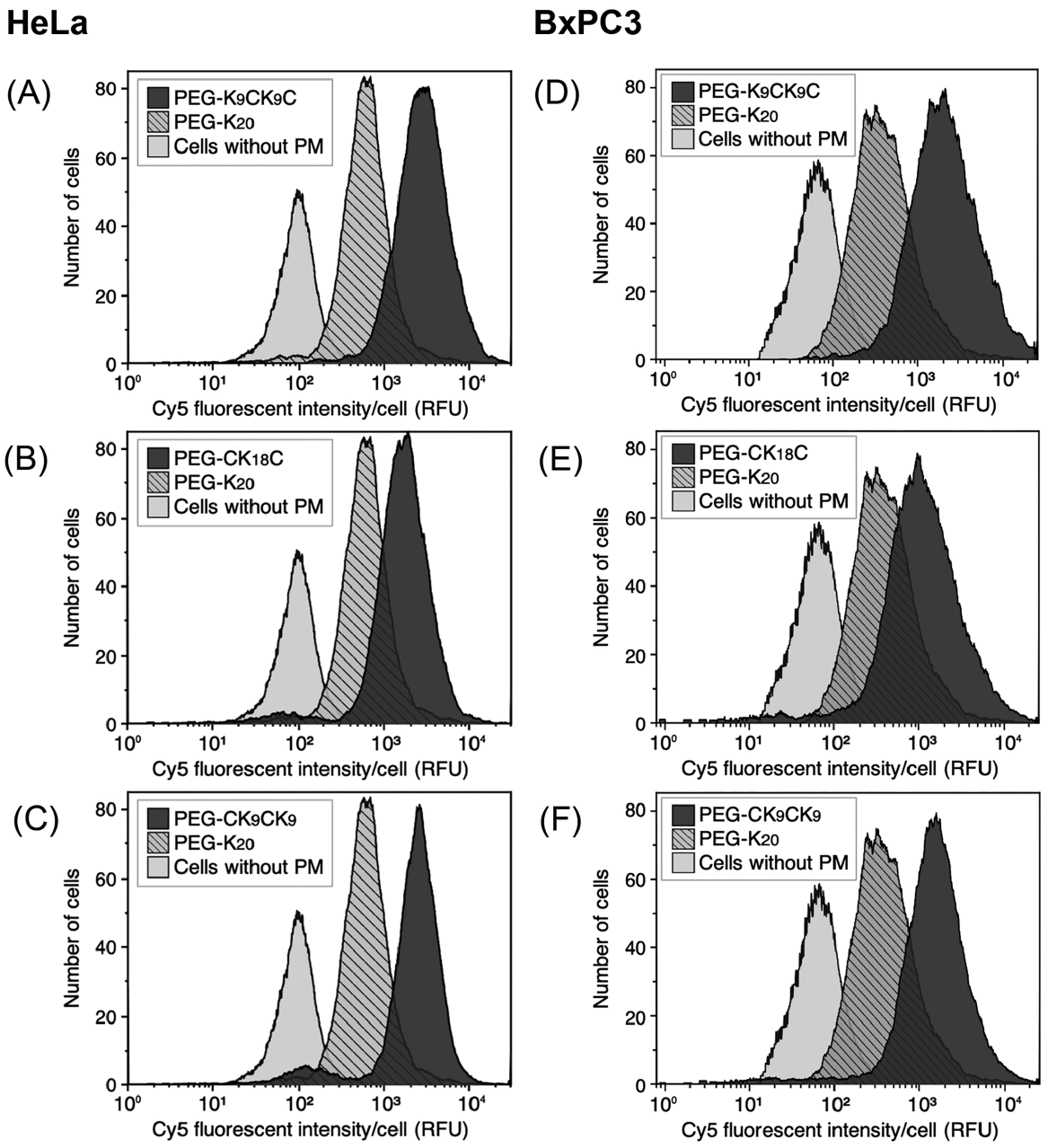

Figure 7. Cellular uptake of PMs loading Cy5-labeled pDNA against HeLa (left) and BxPC3 cell lines (right) examined by flow cytometry. Cellular uptake of the cross-linked PMs composed of PEG−K_9CK_9C (A, D), PEG−$CK_{18}C$ (B, E), and PEG−CK_9CK_9 (C, F) was compared with those of non-cross-linked PMs composed of PEG−K_{20} and cells without the addition of PMs as a control (n = 10 000).

was 10^3-fold higher than that of the most efficient PEG−peptide (PEG−K_9CK_9C) in the luciferase assay using Huh-7 cells. The evaluation of PEI was omitted from the graphical representation.

A considerable enhancement in reporter gene expression was only observed in PEG−K_9CK_9C PMs, despite the presence of minor modulation in other PM-mediated expressions in this study. The previously reported observation that PEG−$CK_{18}C$ PMs[19] mediated the maximum gene expression in HeLa cells seems to be erroneously obtained due to normality-depleted HeLa cells, as described in the Introduction. Generally, a marked difference in gene expression efficacy was observed according to the cell lines employed. The cell-line-dependent magnitude relationship in gene expression can be considered in relation to the differentiation properties of each cell line that can affect cellular activity, i.e., proliferation rate. The population doubling time of PANC-1 and BxPC3 cell lines has been reported to be 54 and 48−60 h, respectively.[29] In fact, these two cell lines showed considerably lower expression than those observed in Huh-7 and HeLa cell lines (Figure 6). HeLa cells that exhibited a generally higher expression possessed a much shorter population doubling time of 24 h.[30] After hypothermic incubation at 4 °C, the reporter gene expression mediated by all PMs was evenly reduced to less than 20% of the normal expression in all cell lines (data not shown).

In Huh-7 and HeLa cells, non-cross-linked PMs composed of PEG−K_{20} exhibited significant expression, demonstrating the superiority of PEG-oligolysines as a platform for synthetic gene delivery carriers. On the other hand, cross-linked PMs

https://doi.org/10.1021/acsomega.2c00122
ACS Omega 2022, 7, 15478−15487

composed of PEG−CK_9CK_9 showed almost equal or lower gene expression than that observed in non-cross-linked PMs in all cell lines, suggesting no advantage in gene expression efficacy. Additionally, for the cross-linked PMs composed of PEG−$CK_{18}C$, higher gene expression than that mediated by PEG−K_{20} was obtained only in the PANC-1 cell line. Therefore, among the cross-linked PMs, it is reasonable to conclude that only PEG−K_9CK_9C PMs had an enhanced gene expression advantage relative to non-cross-linked PMs composed of PEG−K_{20}.

Cellular Uptake of PMs in Different Cell Lines. Finally, we attempted to determine the relationship between the PEG−peptide sequence and gene expression efficacy by comparing cellular uptake and gene expression results. The cellular uptake results of all PMs using HeLa and BxPC3 cell lines are graphically shown in Figure 7. In addition, the values of mean fluorescence intensity corresponding to each panel of Figure 7 are shown in Table 2 as a cell-number-based arithmetic mean (the effect of fluorescence intensity was not considered as a weighting factor in the calculation). In this assay, nontransfected cells were used as controls in each cell line.

Table 2. Mean Fluorescence Intensity for Cellular Uptake Obtained by Flow Cytometry

arithmetic mean	HeLa	BxPC3
PEG−K_9CK_9C	3344	3159
PEG−$CK_{18}C$	2071	1855
PEG−CK_9CK_9	2782	2188
PEG−K_{20}	764	610
cells without PM	111	81

While the difference in gene expression efficacy in these two cell lines was 2 orders of magnitude higher in all the PMs (Figure 6), the amount of cross-linked PMs incorporated into each cell line remained in the same order of magnitude (Table 2). In the polyplex and lipoplex systems, a similar trend in which the range of variations in reporter gene expression was much greater than that in cellular uptake was often reported.[31−33] Interestingly, the amount of non-cross-linked PMs (PEG−K_{20} PMs) taken by each cell line remained consistently lower in the range from 27 to 37% of those of cross-linked PMs composed of PEG−$CK_{18}C$ and PEG−CK_9CK_9 (Table 2), whereas the gene expression efficacy mediated by PEG−K_{20} PMs reached the same level as those of PEG−$CK_{18}C$ PMs and PEG−CK_9CK_9 PMs. Although the use of disulfide-cross-linked vectors that release pDNA in response to the intracellular reductive environment was suggested,[1,10,18,40] the results obtained in this study indicate that it is not always possible for the installation of disulfide cross-linking into PMs to enhance the PM-mediated gene expression.

Let us consider the relationship between PEG density of PMs and cellular uptake. The PEG density on rod-like PMs is obtained by dividing the number of PEG−peptides bound to pDNA by the surface area of the PM core, which was composed of pDNA and peptide segments. For simplicity, when the rod-like PM is treated as a circular cylinder with mean rod length, the surface area of the PM core is given by the sum of the surface of the cylinder side and the area of both ends. In this calculation, the interhelical spacing was assumed to be 3.04 nm according to small-angle X-ray scattering measurement for PLys/DNA complexes.[41] The number of PEG−peptides bound to pDNA was calculated to be 682 for cysteine-installed PEG−peptide PMs and 617 for PEG−K_{20} PMs by assuming charge-neutralized PMs because PM charge neutralization was confirmed by the results of gel electrophoresis (Figures 2 and 5), and almost PMs were suggested to be formulated from single pDNA condensates by the TEM analysis of our previous study.[19] The PEG density on PMs was calculated from the relationship between the surface area of the PM core and the number of PEG−peptides bound to pDNA. As shown in Table 1, the PEG density on cysteine-installed PEG−peptide PMs (cross-linked PMs) was calculated to be sparser than that of PEG−K_{20} PMs (non-cross-linked PMs). Similarly, Tockary et al. reported that longer rod-like PMs have a sparser PEG layer on PEG−PLL PMs.[34]

From the results of PM cellular uptake (Figure 7 and Table 2), the amount of cross-linked PMs taken by each cell line was calculated to be from 2.7- to 5.2-fold higher than that of non-cross-linked PM. Whereas smaller polyplexes are generally known to exhibit higher cellular uptake,[35] the opposite result that the longer PMs were effective in the cellular uptake was obtained in the present study. This fact may relate to the sparser PEG density on the cross-linked PM surface. On the comparison between cross-linked PMs and non-cross-linked PMs, this idea corresponds to the concept of a PEG dilemma.[36] Thus, the sparser PEG density on cross-linked PMs may contribute to the increased cellular uptake of cross-linked PMs.

Considering the gene expression efficacy in detail, PEG−K_9CK_9C PMs seem to have a considerable advantage over other PMs in all cell lines, exhibiting two to eight times the gene expression efficacy of other PMs. However, the amount of cellular uptake of PEG−K_9CK_9C PMs remained only 1.2- to 1.7-fold higher than that mediated by other cross-linked PMs. Therefore, it can be said that PM-mediated gene expression efficacy was not directly affected by the efficacy of cellular uptake of PMs.

In the present study, disulfide cross-links were introduced to improve extracellular PM stability and facilitate pDNA release inside the cells but not to accelerate the gene expression of particular PMs. Although the rod length distributions of cross-linked PMs were not substantially different among them and the robustness of PEG−K_9CK_9C PMs and PEG−$CK_{18}C$ PMs were almost the same, it is unexpected that the slight advantage in cellular uptake of PEG−K_9CK_9C PMs seems to be largely enhanced in synergy with unknown intracellular processes, leading to the resultant maximum gene expression in PEG−K_9CK_9C PMs alone. Further studies including a time dependency of PM-mediated gene expression or the intracellular traffic of PMs should be conducted to clarify the key to this enhancement of intracellular processes.

CONCLUSION

This work was conducted to re-examine the previously reported peptide-sequence-dependent gene expression mediated by double-cysteine-installed PEGylated oligolysines. Cysteine-installed PEG-oligolysines were synthesized to formulate reductive environment-responsive PMs as candidates for artificial gene vectors, which exhibited pDNA release under intracellular reductive conditions. From the physicochemical characterizations, including an EtBr dye exclusion assay, TEM observation, and a gel electrophoresis retardation assay, the reproducibility of PM formation with cysteine-installed PEG-

https://doi.org/10.1021/acsomega.2c00122
ACS Omega 2022, 7, 15478−15487

oligolysines was firmly confirmed. To evaluate bioactivities, luciferase gene expression and cellular uptake were evaluated to elucidate the correlation between these cellular functions. We previously reported that PEG−CK_{18}C PMs mediated the maximum luciferase gene expression in HeLa cells, which was 35-fold higher than that mediated by cysteine-uninstalled PEGylated oligolysine PEG−K_{20}. However, in the present study, the maximum reporter gene expression was observed in PEG−K_9CK_9C PMs in all cell lines assessed. The enhancement in reporter gene expression was 2- to 8-fold higher than that mediated by other PMs. Although maximum cellular uptake was observed in PEG−K_9CK_9C PMs, the differences among all PMs remained in the same order of magnitude. Thus, unknown intracellular processes might enhance the slight advantage in the cellular uptake of PEG−K_9CK_9C PMs, resulting in the observed maximum gene expression in PEG−K_9CK_9C PMs.

■ ASSOCIATED CONTENT

Supporting Information

The Supporting Information is available free of charge at https://pubs.acs.org/doi/10.1021/acsomega.2c00122.

GPC charts of purified protected PEG−peptides, PM stability against DNase or serum, and DLS measurements for PMs prior to and after the incubation in serum (PDF)

■ AUTHOR INFORMATION

Corresponding Author

Yuichi Yamasaki − *Department of Materials Engineering, Graduate School of Engineering, The University of Tokyo, Bunkyo-ku, Tokyo 113-8656, Japan;* orcid.org/0000-0001-8358-6550; Email: nked8330@g.ecc.u-tokyo.ac.jp

Authors

Daiki Kumekawa − *Department of Materials Engineering, Graduate School of Engineering, The University of Tokyo, Bunkyo-ku, Tokyo 113-8656, Japan;* Present Address: Toray Industries, Deguchi, Yahagi-cho, Okazaki 444-8522, Japan

Satoshi Yamauchi − *Department of Materials Engineering, Graduate School of Engineering, The University of Tokyo, Bunkyo-ku, Tokyo 113-8656, Japan;* Present Address: Mizuho Securities, Otemachi First Square, 1-5-1, Chiyoda-ku, Tokyo 100-0004, Japan.

Hodaka Omuro − *Department of Materials Engineering, Graduate School of Engineering, The University of Tokyo, Bunkyo-ku, Tokyo 113-8656, Japan;* Present Address: Nippon Steel Corporation, 2-6-1, Marunouchi, Chiyoda-ku, Tokyo 100-8071, Japan.

Complete contact information is available at: https://pubs.acs.org/10.1021/acsomega.2c00122

Author Contributions

Y.Y. organized the study and wrote the manuscript. D.K., S.Y., and H.O. performed experiments. All authors reviewed the manuscript.

Notes

The authors declare no competing financial interest.

■ ACKNOWLEDGMENTS

We thank Ms. Satomi Ogura for technical advice on the gene expression assay. A part of this work was supported by JST COI Grant Number JPMJCE1305. ESI-MS and flow cytometry were performed at the One-stop Sharing Facility Center for Future Drug Discoveries in Graduate School of Pharmaceutical Sciences, the University of Tokyo. TEM observation was conducted at the Advanced Characterization Nanotechnology Platform of the University of Tokyo, supported by the "Nanotechnology Platform" of the Ministry of Education, Culture, Sports, Science and Technology (MEXT), Japan.

■ ABBREVIATIONS

PEG	poly(ethylene glycol)
PM	polyplex micelle
pDNA	plasmid DNA
TEM	transmission electron microscope
PLL	poly-L-lysines
DP	degree of polymerization
NCA	*N*-carboxy anhydride
SPPS	solid-phase peptide synthesis

■ REFERENCES

(1) Park, Y.; Kwok, K. Y.; Boukarim, C.; Rice, K. G. Synthesis of sulfhydryl cross-linking poly(ethylene glycol)-peptides and glycopeptides as carriers for gene delivery. *Bioconjugate Chem.* **2002**, *13*, 232−239.

(2) Baumhover, N. J.; Duskey, J. T.; Khargharia, S.; White, C. W.; Crowley, S. T.; Allen, R. J.; Rice, K. G. Structure−activity relationship of PEGylated polylysine peptides as scavenger receptor inhibitors for non-viral gene delivery. *Mol. Pharmaceutics* **2015**, *12*, 4321−4328.

(3) Kwok, K. Y.; McKenzie, D. L.; Evers, D. L.; Rice, K. G. Formulation of highly soluble poly(ethylene glycol)-peptide DNA condensates. *J. Pharm. Sci.* **1999**, *88*, 996−1003.

(4) Wolfert, M. A.; Schacht, E. H.; Toncheva, V.; Ulbrich, K.; Nazarova, O.; Seymour, L. W. Characterization of vectors for gene therapy formed by self-assembly of DNA with synthetic block copolymers. *Hum. Gene Ther.* **1996**, *7*, 2123−2133.

(5) Katayose, S.; Kataoka, K. Water-soluble polyion complex associates of DNA and poly(ethylene glycol)-poly(L-lysine) block copolymer. *Bioconjugate Chem.* **1997**, *8*, 702−707.

(6) Männistö, M.; Vanderkerken, S.; Toncheva, V.; Elomaa, M.; Ruponen, M.; Schacht, E.; Urtti, A. Structure−activity relationships of poly(L-lysines): effects of pegylation and molecular shape on physicochemical and biological properties in gene delivery. *J. Controlled Release* **2002**, *83*, 169−182.

(7) Abdallah, B.; Sachs, L.; Demeneix, B. A. Non-viral gene transfer: Application in developmental biology and gene therapy. *Biol. Cell* **1995**, *85*, 1−7.

(8) Liu, Q.; Muruve, D. A. Molecular basis of the inflammatory response to adenovirus vectors. *Gene Ther.* **2003**, *10*, 935−940.

(9) Collard, W. T.; Yang, Y.; Kwok, K. Y.; Park, Y.; Rice, K. G. Biodistribution, metabolism, and *in vivo* gene expression of low molecular weight glycopeptide polyethylene glycol peptide DNA cocondensates. *J. Pharm. Sci.* **2000**, *89*, 499−512.

(10) Yang, Y.; Park, Y.; Man, S.; Liu, Y.; Rice, K. G. Cross-linked low molecular weight glycopeptide-mediated gene delivery: Relationship between DNA metabolic stability and the level of transient gene expression *in vivo*. *J. Pharm. Sci.* **2001**, *90*, 2010−2022.

(11) Kagaya, H.; Oba, M.; Miura, Y.; Koyama, H.; Ishii, T.; Shimada, T.; Takato, T.; Kataoka, K.; Miyata, T. Impact of polyplex micelles installed with cyclic RGD peptide as ligand on gene delivery to vascular lesions. *Gene Ther.* **2012**, *19*, 61−69.

(12) Martin, M. E.; Rice, K. G. Peptide-guided gene delivery. *AAPS J.* **2007**, *9*, E18−E29. and references therein

(13) Smith, L. C.; Duguid, J.; Wadhwa, M. S.; Logan, M. J.; Tung, C.−H.; Edwards, V.; Sparrow, J. T. Synthetic peptide-based DNA complexes for nonviral gene delivery. *Adv. Drug Delivery Rev.* **1998**, *30*, 115−131. and references therein
(14) Cheng, J.; Deming, T. J. Synthesis of polypeptides by ring-opening polymerization of α-amino acid N-carboxyanhydrides. *Top. Curr. Chem.* **2011**, *310*, 1−26.
(15) Wagner, E.; Cotten, M.; Foisner, R.; Birnstiel, M. L. Transferrin-polycation-DNA complexes: The effect of polycations on the structure of the complex and DNA delivery to cells. *Proc. Natl. Acad. Sci. U. S. A.* **1991**, *88*, 4255−4259.
(16) Canine, B. F.; Wang, Y.; Hatefi, A. Evaluation of the effect of vector architecture on DNA condensation and gene transfer efficiency. *J. Controlled Release* **2008**, *129*, 117−123.
(17) Zhou, J.; Li, Y.; Dong, H.; Yuan, H.; Ren, T.; Li, Y. Effect of monomer sequence of poly(histidine/lysine) catiomers on gene packing capacity and delivery efficiency. *RSC Adv.* **2015**, *5*, 14138−14146.
(18) Read, M. L.; Singh, S.; Ahmed, Z.; Stevenson, M.; Briggs, S. S.; Oupicky, D.; Barrett, L. B.; Spice, R.; Kendall, M.; Berry, M.; Preece, J. A.; Logan, A.; Seymour, L. W. A versatile reducible polycation-based system for efficient delivery of a broad range of nucleic acids. *Nucleic Acids Res.* **2005**, *33*, No. e86.
(19) Ueno, M.; Yamauchi, S.; Kumekawa, D.; Yamasaki, Y. Peptide sequence-dependent gene expression of PEGylated peptide/DNA complexes. *Mol. Pharmaceutics* **2019**, *16*, 3072−3082.
(20) Ellman, G. L. Tissue sulfhydryl groups. *Arch. Biochem. Biophys.* **1959**, *82*, 70−77.
(21) Rasband, W. S. *Image J*; U.S. National Institutes of Health: Bethesda, Maryland, USA, 1997−2018; https://imagej.nih.gov/ij/.
(22) Murayama, Y.; Sakamaki, Y.; Sano, M. Elastic response of single DNA molecules exhibits a reentrant collapsing transition. *Phys. Rev. Lett.* **2003**, *90*, 018102.
(23) Besteman, K.; Van Eijk, K.; Lemay, S. G. Charge inversion accompanies DNA condensation by multivalent ions. *Nat. Phys.* **2007**, *3*, 641−644.
(24) Namork, E.; Johansen, B. V. Electron microscopy of nucleic acids: the effect of different post-treatments on contour-length measurements. *Micron* **1980**, *11*, 85−90.
(25) Ruponen, M.; Yla-Herttuala, S.; Urtti, A. Interactions of polymeric and liposomal gene delivery systems with extracellular glycosaminoglycans: physicochemical and transfection studies. *Biochim. Biophys. Acta Biomembrane* **1999**, *1415*, 331−341.
(26) Xu, Y.; Szoka, F. C., Jr. Mechanism of DNA release from cationic liposome/DNA complexes used in cell transfection. *Biochemistry* **1996**, *35*, 5616−5623.
(27) Zuckerman, J. E.; Choi, C. H. J.; Han, H.; Davis, M. E. Polycation-siRNA nanoparticles can disassemble at the kidney glomerular basement membrane. *Proc. Natl. Acad. Sci. U. S. A.* **2012**, *109*, 3137−3142.
(28) Burke, R. S.; Pun, S. H. Extracellular barriers to in vivo PEI and PEGylated PEI polyplex mediated gene delivery to the liver. *Bioconjugate Chem.* **2008**, *19*, 693−704.
(29) Deer, E. L.; Gonzalez-Hernandez, J.; Coursen, J. D.; Shea, J. E.; Ngatia, J.; Scaife, C. L.; Firpo, M. A.; Mulvihill, S. J. Phenotype and genotype of pancreatic cancer cell lines. *Pancreas* **2010**, *39*, 425−435.
(30) Zocchi, E.; Daga, A.; Usai, C.; Franco, L.; Guida, L.; Bruzzone, S.; Costa, A.; Marchetti, C.; De Flora, A. Expression of CD38 increases intracellular calcium concentration and reduces doubling time in HeLa and 3T3 cells. *J. Biol. Chem.* **1998**, *273*, 8017−8024.
(31) Haensler, J.; Szoka, F. C., Jr. Polyamidoamine cascade polymers mediate efficient transfection of cells in culture. *Bioconjugate Chem.* **1993**, *4*, 372−379.
(32) Tang, M. X.; Szoka, F. C., Jr. The influence of polymer structure on the interactions of cationic polymers with DNA and morphology of the resulting complexes. *Gene Ther.* **1997**, *4*, 823−832.
(33) Zabner, J.; Fasbender, A. J.; Moninger, T.; Poellinger, K.; Welsh, M. J. Cellular and molecular barriers to gene transfer by a cationic lipid. *J. Biol. Chem.* **1995**, *270*, 18997−19007.
(34) Tockary, T. A.; Osada, K.; Chen, Q.; Machitani, K.; Dirisala, A.; Uchida, S.; Nomoto, T.; Toh, K.; Matsumoto, Y.; Itaka, K.; Nitta, K.; Nagayama, K.; Kataoka, K. Tethered PEG crowdedness determining shape and blood circulation profile of polyplex micelle gene carriers. *Macromolecules* **2013**, *46*, 6585−6592.
(35) Mathew, B.; Ramanathan, R.; Delvaux, N. A.; Poliskey, J.; Rice, K. G. Heat-shrinking DNA nanoparticles for in vivo gene delivery. *Gene Ther.* **2020**, *27*, 196−208.
(36) Hatakeyama, H.; Akita, H.; Kogure, K.; Oishi, M.; Nagasaki, Y.; Kihira, Y.; Ueno, M.; Kobayashi, H.; Kikuchi, H.; Harashima, H. Development of a novel systemic gene delivery system for cancer therapy with a tumor-specific cleavable PEG-lipid. *Gene Ther.* **2007**, *14*, 68−77.
(37) Ziady, A.-G.; Gedeon, C. R.; Miller, T.; Quan, W.; Payne, J. M.; Hyatt, S. L.; Fink, T. L.; Muhammad, O.; Oette, S.; Kowalczyk, T.; Pasumarthy, M. K.; Moen, R. C.; Cooper, M. J.; Davis, P. B. Transfection of Airway Epithelium by Stable PEGylated Poly-L-lysine DNA Nanoparticles in Vivo. *Mol. Ther.* **2003**, *8*, 936−947.
(38) Harmon, B. T.; Aly, A. E.; Padegimas, L.; Sesenoglu-Laird, O.; Cooper, M. J.; Waszczak, B. L. Intranasal administration of plasmid DNA nanoparticles yields successful transfection and expression of a reporter protein in rat brain. *Gene Ther.* **2014**, *21*, 514−521.
(39) Konstan, M. W.; Davis, P. B.; Wagener, J. S.; Hilliard, K. A.; Stern, R. C.; Milgram, L. J.H.; Kowalczyk, T. H.; Hyatt, S. L.; Fink, T. L.; Gedeon, C. R.; Oette, S. M.; Payne, J. M.; Muhammad, O.; Ziady, A. G.; Moen, R. C.; Cooper, M. J. Compacted DNA nanoparticles administered to the nasal mucosa of cystic fibrosis subjects are safe and demonstrate partial to complete cystic fibrosis transmembrane regulator reconstitution. *Hum. Gene Ther.* **2004**, *15*, 1255−1269.
(40) Ward, C. M.; Pechar, M.; Oupicky, D.; Ulbrich, K.; Seymour, L. W. Modification of pLL/DNA complexes with a multivalent hydrophilic polymer permits folate-mediated targeting in vitro and prolonged plasma circulation in vivo. *J. Gene Med.* **2002**, *4*, 536−547.
(41) DeRouchey, J.; Netz, R. R.; Rädler, J. O. Structural investigations of DNA-polycation complexes. *Eur. Phys. J. E* **2005**, *16*, 17−28.
(42) Flory, P. J. *Principles of Polymer Chemistry*; Cornell University Press: Ithaca, NY, 1953.
(43) Rüegg, U. T.; Rudinger, J. Reductive cleavage of cystine disulfides with tributylphosphine. *Methods Enzymol* **1977**, *47*, 111−116.

https://doi.org/10.1021/acsomega.2c00122
ACS Omega 2022, 7, 15478−15487